RHEOLOGICAL MODELISATION OF A STRUCTURAL BOND : INFLUENCE OF THE INERTIA

Pacs Reference : 43.35.Zc

Valentina Vlasie, Martine Rousseau
Laboratoire de Modélisation en Mécanique, Université Paris 6, UMR CNRS 7607 case 162
8 rue du Capitaine Scott, 75015 Paris, France
Tel : 01 44 27 87 16
Fax : 01 44 27 52 59
E-mail : vlasie@lmm.jussieu.fr; mrousse@ccr.jussieu.fr

ABSTRACT
We want to test by ultrasonic waves the adhesion of an aluminum/adhesive/aluminum structural bond. Thus, we compare the guided modes for the tri-layer model and a rheological model of the adhesive layer (geometrical interface with a uniform distribution of springs with mass). A comparison between the two models shows a good agreement for the adhesive thickness smaller than a characteristic value and allows us to define the stiffnesses and the mass of the springs.

1. INTRODUCTION

In the literature, rheological models are used to modelize the tri-layer interfaces [Mal, 1989], [Rocklin, 1991], [Kundu, 1997]. In this paper, we want to study the influence of the inertia on the validity limits of such models. Firstly, we consider the exact model, i. e. a tri-layer with continuity of stresses and displacements at each interface. Secondly, we modelize the adhesive layer by a uniform distribution of longitudinal and transversal springs with mass. Then, the boundary conditions at the interfaces are the springs-mass conditions. The parameters of the adhesion are the stiffnesses and the mass of the springs. A dispersion curves comparison shows the existence of a relative adhesive-thickness value beyond which the springs-mass rheological model is not sufficient to modelize the tri-layer. A cutoff-frequencies comparison shows a frequency dependence of stiffnesses and mass. This dependence is unusual and means that the rheological model must be adapted according to the considered frequency range. In particular, for small relative adhesive-thicknesses or/and low frequency, we find the definition of stiffness constants and mass used in the literature.

2. TRI-LAYER MODEL

We consider a tri-layer structure composed of two identical metallic plates (S_1, S_3) joined by an adhesive (S_2). We denote ρ_i the mass density of i-medium ($i=1,2$), c_{Li} the corresponding longitudinal wave velocity, c_{Ti} the transversal wave velocity, $2h$ the thickness of S_1 and S_3 and d the thickness of S_2. The structure being symmetrical, we were only interested by the substructure $S_1 - S_2$. We consider the case of plane deformations in the Oxz plane (Ox-axis is the medium line of

S_1 and oz-axis is taken positive up-down). In plane deformations, the scalar potential and the unique component of the vectorial potential are written, for the S_1 and S_2 layers:

$$\phi_1 = \left[A_{1L}\cos(k_{Lz1}z) + B_{1L}\sin(k_{Lz1}z)\right]e^{i(k_x x-\omega t)}$$
$$\psi_1 = \left[A_{1T}\cos(k_{Tz1}z) + B_{1T}\sin(k_{Tz1}z)\right]e^{i(k_x x-\omega t)},$$
$$\phi_2 = B_{2L}\left[R^L e^{ik_{Lz2}(z-h)} + e^{-ik_{Lz2}(z-h)}\right]e^{i(k_x x-\omega t)}$$
$$\psi_2 = B_{2T}\left[R^T e^{ik_{Tz2}(z-h)} + e^{ik_{Tz2}(z-h)}\right]e^{i(k_x x-\omega t)},$$

where R^L and R^T, the reflection coefficients of the longitudinal and transversal waves inside the adhesive layer, are given by :

$$R^L = \pm e^{-ik_{Lz2}d}\ ,\ R^T = \pm e^{-ik_{Tz2}d}.$$

The boundary conditions are the free surface conditions at $z=-h$, the continuity of stresses and displacements at the $z=h$. At $z=h+d$ and taking into account the structure symmetry, the boundary conditions are substituted by R^L and R^T coefficients. Thus, we obtain a 6×6 system in which the zeros of the determinant correspond to the guided waves into the structure. This system depends on R^L and R^T so we obtain four characteristic equations, defining four families of dispersion curves, respectively denoted (-,-), (-,+), (+,-) and (+,+), where the first sign in the parenthesis represents the sign of R^L and the second one, the sign of R^T.

We introduce the dimensionless quantities: $\bar{\omega} = 2k_e h$, $\overline{k_x} = k_x/k_e$, $\overline{k_{Lzi}} = k_{Lzi}/k_e$, $\overline{k_{Tzi}} = k_{Tzi}/k_e$ and the notations $n_{Li} = k_{Li}/k_e$, $z_L = \rho_1 c_{L1}/\rho_2 c_{L2}$, $z_T = \rho_1 c_{T1}/\rho_2 c_{T2}$ (i=1,2). The wave number k_e is defined by $k_e = \omega/c_{water}$. This choice is made for two reasons: (i) no waves in the structure are accorded any privilege, (ii) the definition of the dimensionless quantities may be extended to the case of the immersed structure.

When $\overline{k_x} = 0$, the characteristic equations are simplified. Therefore, we obtain the cutoff-frequencies as solutions of:

$$\cos(n_{L1}\bar{\omega}) - z_L\, tg\left(n_{L2}\bar{\omega}d/4h\right)\sin(n_{L1}\bar{\omega}) = 0,$$
$$\cos(n_{L1}\bar{\omega}) + z_L\cot g\left(n_{L2}\bar{\omega}d/4h\right)\sin(n_{L1}\bar{\omega}) = 0,$$

$$\cos(n_{T1}\bar{\omega}) - z_T\, tg\left(n_{T2}\bar{\omega}d/4h\right)\sin(n_{T1}\bar{\omega}) = 0,$$
$$\cos(n_{T1}\bar{\omega}) + z_T\cot g\left(n_{T2}\bar{\omega}d/4h\right)\sin(n_{T1}\bar{\omega}) = 0.$$

For an aluminum/epoxy/aluminum tri-layer with the acoustical characteristics $c_{L1}=6380\mathrm{m/s}$, $c_{T1}=3100\mathrm{m/s}$, $\rho_1=2800\mathrm{kg/m^3}$, $c_{L2}=1882\mathrm{m/s}$, $c_{T2}=1086\mathrm{m/s}$, $\rho_2=1160\mathrm{kg/m^3}$ and $c_{water}=1500\mathrm{m/s}$, the dispersion curves are plotted between $\bar{\omega}\in(0,20)$ and $\overline{k_x}\in(0,1)$. Their behavior depends on the parameter $d/2h$.

- For $d/2h$ between 10^{-5} and $3.5\,10^{-2}$, the adhesive layer is negligible and the acoustical waves "see" only a $4h$ thickness aluminum plate. The cutoff-frequencies remain relatively around those of a $4h$ thickness aluminum plate and, for $\overline{k_x}\neq 0$, there is an undoubling of modes.

The curves of the (-,-) family are almost fixed when $d/2h$ varies. They correspond to the dispersion curves of a $2h$ thickness aluminum plate. The curves of (+,-) and (-,+) families get closer to those of a $4h$ thickness aluminum plate. The (+,+) family curves are specific to the tri-layer.

- For $d/2h$ between $3.5\,10^{-2}$ and $2\,10^{-1}$, the adhesive thickness is significant enough to isolate the two aluminum plates as well as assure their coupling. The cutoff-frequencies are now centered around

those of a $2h$ thickness aluminum plate. We still observe, from every cutoff and for $\overline{k_x} \neq 0$, an undoubling of modes. In fact, the doubles are two by two regrouped around one mode of a $2h$ thickness aluminum plate. These regroupings may be interpreted as a quadrupling of modes around the $2h$ thickness aluminum plate modes (see figure 1).
Moreover, at low frequency, we observe two doubles, one longitudinal and another transversal, whose specificity is that one of their dispersion curves is vertical for weak angles of propagation, so we name them vertical modes. The interest of these modes is essentially experimental because of their low angular sensibility. A longitudinal vertical mode had already be observed for an aluminum/water/aluminum tri-layer [Lenoir, 1997].

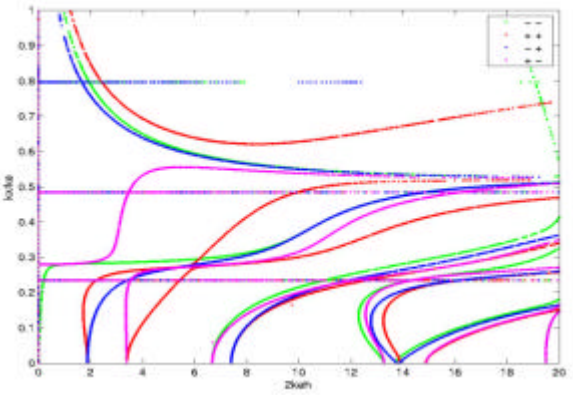

Figure 1 – Dispersion curves of a tri-layer structure for $d/2h = 10^{-1}$.

• For $d/2h$ tending towards 1, the adhesive layer has progressively the same role as that of the aluminum plates. The quadrupling disappears and the dispersion curves are more complex, in particular, the Lamb modes of the adhesive layer begin to be observed.

3. SPRINGS MODEL WITH INERTIA

We consider the same tri-layer structure as before but the S_2-adhesive layer is now substituted by a geometrical surface $z = 0$ and the adhesion process is modelized by an uniform distribution of longitudinal and transversal springs with inertia. We respectively denote their stiffnesses by K_L^m and K_T^m and their mass by m.

As previously, the components of the potentials are written, for the S_1 and S_3 layers:

$$\begin{aligned}
\phi_1 &= \left[A_{1L}\cos\left(k_{Lz1}(z+h)\right) + B_{1L}\sin\left(k_{Lz1}(z+h)\right)\right]e^{i(k_x x-\omega t)} \\
\psi_1 &= \left[A_{1T}\cos\left(k_{Tz1}(z+h)\right) + B_{1T}\sin\left(k_{Tz1}(z+h)\right)\right]e^{i(k_x x-\omega t)} \\
\phi_3 &= \left[A_{3L}\cos\left(k_{Lz1}(z-h)\right) + B_{3L}\sin\left(k_{Lz1}(z-h)\right)\right]e^{i(k_x x-\omega t)} \\
\psi_3 &= \left[A_{3T}\cos\left(k_{Tz1}(z-h)\right) + B_{3T}\sin\left(k_{Tz1}(z-h)\right)\right]e^{i(k_x x-\omega t)}
\end{aligned},$$

The boundary conditions require to obtain the dispersion equation are the free surface conditions at $z = \pm 2h$ and at $z = 0$, we must write:

$$\sigma_{xz1} = K_T^m(u_x^3 - u_x^1) - m\frac{d^2u_x^{int}}{dt^2},\ \sigma_{xz3} = K_T^m(u_x^3 - u_x^1) + m\frac{d^2u_x^{int}}{dt^2},$$

$$\sigma_{zz1} = K_L^m(u_z^3 - u_z^1) - m\frac{d^2u_z^{int}}{dt^2},\ \sigma_{zz3} = K_L^m(u_z^3 - u_z^1) + m\frac{d^2u_z^{int}}{dt^2},$$

where $\left[u_x^1, 0, u_z^1\right]$, $\left[u_x^3, 0, u_z^3\right]$ and $\left[u_x^{int}, 0, u_z^{int}\right]$ are respectively the displacement vectors in S_1, S_3 and of the mass m.

Thus, we obtain a 8×8 system, in which the roots of the determinant yield the guided modes into the structure. For numerical calculation, we introduce the same dimensionless quantities as before, to which we add the following: $\overline{K_L^m} = K_L^m (2h/(\lambda_1 + 2\mu_1))$, $\overline{K_T^m} = K_T^m (2h/\mu_1)$ and $\overline{m} = m/2\rho_1 h$.

If $\overline{k_x} = 0$, the dispersion equation may be factorized in two parts (one transversal and another longitudinal) that give the cutoff-frequencies of the guided waves.

$$\left(-n_{T1}\overline{\omega}s_{T1} + \overline{K_T^m}c_{T1}\right)\left(s_{T1} + \left(-n_T\overline{\omega}s_{T1} + \overline{K_T^m}c_{T1}\right)\overline{\omega}n_T\overline{m}/\left(2\overline{K_T^m}\right)\right) = 0,$$

$$\left(-n_L\overline{\omega}s_{L1} + \overline{K_L^m}c_{L1}\right)\left(s_{L1} + \left(-n_L\overline{\omega}s_{L1} + \overline{K_L^m}c_{L1}\right)\overline{\omega}n_L\overline{m}/\left(2\overline{K_L^m}\right)\right) = 0,$$

where $s_{T1,L1} = \sin\left(\overline{\omega}n_{T1,L1}\right)$ and $c_{T1,L1} = \cos\left(\overline{\omega}n_{T1,L1}\right)$.

We remark that the first parenthesis only depends on the spring stiffnesses. The second one principally depends on the mass so, if we set $\overline{m} = 0$, we find the rheological model without mass [Vlasie, 2002].

The dispersion curves are presented for two aluminum plates and plotted between $\overline{\omega} \in (0, 20)$ and $\overline{k_x} \in (0,1)$. The behavior of the dispersion curves depends on the stiffnesses and the mass of the springs. To illustrate their form we present the dispersion curves for $\overline{K_L^m} = 0.4$, $\overline{K_T^m} = 0.4$ and $\overline{m} = 0.0527$ (figure 2). We notice an undoubling of modes around these of a $2h$ thickness aluminum plate. Moreover, at low frequency, we observe two vertical modes, one longitudinal and another transversal.

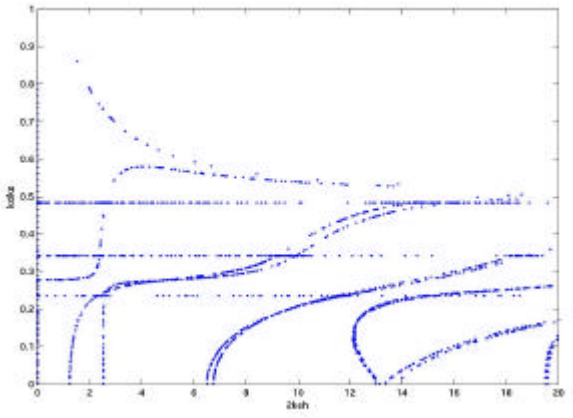

Figure 2 - Dispersion curves for $\overline{K_L^m} = 0.4$, $\overline{K_T^m} = 0.4$ and $\overline{m} = 0.0527$.

4. COMPARISON BETWEEN THE TWO MODELS

The comparison between the cutoff-frequencies equations of the two models gives:

$$\overline{K_{L,T\,exact}^m} = \overline{\omega}n_{L1,T1}/\left(2z_{L,T}\right)\cot\left(\overline{\omega}n_{L2,T2}\,d/4h\right),$$
$$\overline{m}_{exact} = 2/\left[\overline{\omega}n_{L1,T1}\left(\overline{\omega}n_{L1,T1}/\overline{K_{L,T}^m} + z_{L,T}\cot(\overline{\omega}n_{L2,T2}d/4h)\right)\right].$$

We observe a frequency dependence of parameters which means that the rheological model must be adapted according to the considered frequency range. Moreover, we observe that the longitudinal and transversal springs do not have the same mass. Initially we do not have considered this case but the decoupling effect at $\overline{k_x} = 0$ allows us to find this result. We also notice that the longitudinal and transversal masses depend on the corresponding stiffnesses.

When the cotangent argument is smaller then unity (which is verified when $d/2h << 1$ and/or $\overline{\omega} << 1$), a first order expansion gives: $\overline{K^m_{L\ app}} = 2\dfrac{(\lambda_2 + 2\mu_2)/d}{(\lambda_1 + 2\mu_1)/2h}$, $\overline{K^m_{T\ app}} = \dfrac{\mu_2/d}{\mu_1/2h}$ and $\overline{m}_{app} = \dfrac{\rho_2 d}{\rho_1 2h}$. In this case we find the definition of the stiffness constants and mass used in the literature [Rocklin, 1991].

Thus, for $d/2h \in \left(10^{-5}, 3.5\,10^{-2}\right)$ and $\overline{\omega} \in (0,20)$ a good agreement between the guided modes of the springs model with mass and the families (-,+) and (+,-) of the tri-layer model is obtained using approached values of the parameters and we can define an uniform rheological model for this frequency range.

For $d/2h \in \left(3.5\,10^{-2}, 2\,10^{-1}\right)$ and $\overline{\omega} \in (0,20)$ the agreement using the approached values is reduced at the two modes which have the same cutoff-frequencies as the vertical modes. For the other modes, it is necessary to consider exact values of the rheological parameters. For some frequency ranges, the cotangent function assumes negative values and it is not possible to define, even locally, a rheological model.

For $d/2h$ tending towards 1, the dispersion curves of the two models progressively diverge and it becomes difficult to define rheological model even for the low frequency modes.

We have seen that half of the cutoff-frequencies only depends on the stiffnesses and the other half depends on the masses. In the table 1, we compare the exact model with the modes depending on the stiffness $\overline{K^m_L}$. In the table 2, we compare the tri-layer model with the modes depending of the mass $\overline{m_T}$. The numerical results show the differences between the cutoff-frequencies values calculated using the exact and the approximated values of the stiffnesses respectively the masses.

5. CONCLUSIONS

We have modelized an aluminum/adhesive/aluminum structure. We have compared the guided modes, especially their cutoff-frequency for the rheological model with mass and the tri-layer model.

Table 1 – Influence of the exact expression of the stiffness constant upon the cutoff-frequencies

Tri-layer model		Rheological model with mass			
$d/2h$	$\overline{\omega}_{tri-layer}$	$\overline{K^m_{L\ exact}}$	$\overline{\omega}_{exact}$	$\overline{K^m_{L\ app}}$	$\overline{\omega}_{app}$
10^{-5}	6.6805	7212.2	6.6805	7212.2	6.6805
10^{-4}	6.6722	721.22	6.6722	721.22	6.6722
10^{-3}	6.5900	72.122	6.5900	72.122	6.5900
10^{-3}	19.7704	72.122	19.7704	72.122	19.7704
10^{-2}	5.8762	7.2122	5.8760	7.2122	5.8763
10^{-2}	17.8042	7.2102	17.8044	7.2122	17.8071
10^{-1}	3.2235	0.7172	3.2236	0.7212	3.2306
10^{-1}	14.1733	0.6428	14.1734	0.7212	14.2638
$2.5\ 10^{-1}$	2.1648	0.2840	2.1651	0.2884	2.1802
$2.5\ 10^{-1}$	13.4832	0.0898	13.4832	0.2884	13.7415
$4\ 10^{-1}$	1.7322	0.1758	1.7329	0.1804	1.7541
$4\ 10^{-1}$	13.0708	negative	-	0.1804	13.6025

Table 2 – Influence of the exact expression of the mass upon the cutoff-frequencies

Tri-layer model			Rheological model with mass				
$d/2h$	$\bar{\omega}_{tri-layer}$		$\bar{m}_{exact}$	$\bar{\omega}_{exact}$	$\overline{K^{m}_{T,L\ app}}$	$\bar{m}_{app}$	$\bar{\omega}_{app}$
10^{-5}	6.4936		$0.414\ 10^{-5}$	6.4936	10182	$0.414\ 10^{-5}$	6.4936
10^{-5}	12.9871		$0.414\ 10^{-5}$	12.9871	10182	$0.414\ 10^{-5}$	12.9871
10^{-5}	19.4807		$0.414\ 10^{-5}$	19.4807	10182	$0.414\ 10^{-5}$	19.4807
10^{-4}	6.4934		$0.414\ 10^{-4}$	6.4934	1018.2	$0.414\ 10^{-4}$	6.4934
10^{-4}	12.9868		$0.414\ 10^{-4}$	12.9868	1018.2	$0.414\ 10^{-4}$	12.9868
10^{-4}	19.4803		$0.414\ 10^{-4}$	19.4803	1018.2	$0.414\ 10^{-4}$	19.4803
10^{-3}	6.4922		$0.414\ 10^{-3}$	6.4922	101.82	$0.414\ 10^{-3}$	6.4922
10^{-3}	12.9845		$0.414\ 10^{-3}$	12.9845	101.82	$0.414\ 10^{-3}$	12.9845
10^{-3}	19.4765		$0.414\ 10^{-3}$	19.4765	101.82	$0.414\ 10^{-3}$	19.4765
10^{-2}	6.4802		$0.410\ 10^{-2}$	6.4802	10.182	$0.414\ 10^{-2}$	6.4801
10^{-2}	12.9602		$0.410\ 10^{-2}$	12.9602	10.182	$0.414\ 10^{-2}$	12.9601
10^{-2}	19.4402		$0.410\ 10^{-2}$	19.4402	10.182	$0.414\ 10^{-1}$	19.4398
10^{-1}	6.3551		0.0376	6.3493	1.0182	$0.414\ 10^{-1}$	6.3320
10^{-1}	12.6335		0.0298	12.5829	1.0182	$0.414\ 10^{-1}$	12.1758
10^{-1}	18.5472		0.0231	18.108	1.0182	$0.414\ 10^{-1}$	15.13
$2.5\ 10^{-1}$	5.998		0.0614	5.999	0.4072	0.1036	5.2273
$2.5\ 10^{-1}$	9.2915		0.0411	9.2936	0.4072	0.1036	7.1684
$2.5\ 10^{-1}$	13.32		negative	-	0.4072	0.1036	13.1505
$4\ 10^{-1}$	5.0629		0.0754	5.0635	0.2546	0.1657	3.5805
$4\ 10^{-1}$	7.1653		0.0542	7.1645	0.2546	0.1657	6.7206
$4\ 10^{-1}$	16.8986		0.0075	16.9347	0.2546	0.1657	13.0771
$4\ 10^{-1}$	19.799		0.0067	19.7979	0.2546	0.1657	19.5384

The comparison between the dispersion curves allows us to deduce the validity limits of the rheological model. The analytical shape of solutions may be studied as a function of springs stiffnesses and mass. A comparison between the equations that give the cutoff-frequencies for the two models allows us to define the equivalent stiffnesses and masses, both of which are frequency dependent. This dependence means that the rheological model must be adapted to the considered frequency range. A theoretical/experimental comparison is planned. It would consist of evaluating the spring stiffnesses and maybe the masses. A comparison with the exact values of these parameters is interesting for the quality estimation of the interfaces and for the initiation of numerical simulations of the interface damages [Champaney, 2001].

6. BIBLIOGRAPHIE

1. J. P. Jones, J. S. Whittier, *Waves at flexibly bonded interface*, J. Apply. Mech. **December**, 905-908 (1967).

2. A. K. Mal, P. C. Xu and Y. Bar-Cohen, *Analysis of leaky Lamb waves in bonded plates*, Int. J. Engng. Sci, Vol. **27**, No. **7**, pp. 779-791 (1989).

3. S. I. Rockhlin, Y. J. Wang, *Analysis of boundary conditions for elastic wave interaction with an interface between two solids*, J. Acoust. Soc. Am. **89**, 503-515 (1991).

4. O. Lenoir, JL. Izbicki, M. Rousseau, F. Coulouvrat, *Subwavelenght ultrasonic measurement of a very thin fluid layer thickness in a trilayer*, Ultrasonics **35**, 509-515 (1997).

5. T. Kundu and K. Maslov, *Material interface inspection by lamb waves*, Int. J. Solids Structures, Vol. **34**, No. **29**, pp. 3885-3901 (1997).

6. L. Champaney, N. Valoroso, *Numerical evaluation of interface models for the analysis of adhesively bonded joints*, ECCM, European Conference on Computational Mechanics, Cracovie, Pologne (2001).

7. V. Vlasie, M. Rousseau, *Validation acoustique du modèle de ressorts pour l'étude d'un collage structural*, CFA, 6e Congrès Français d'Acoustique, Lille, France (2002).